Condensed Mode Cooling for Ethylene Polymerization: Part V-Reduction of the Crystallization Rate of HDPE in the Presence of Induced Condensing Agents

Fabiana Andrade, René Fulchiron, Franck Collas, Timothy Mckenna

DOI: 10.1002/marc.((insert number)) ((or ppap., mabi., macp., mame., mren., mats.))

Full Paper

Condensed Mode Cooling for Ethylene Polymerization: Part V. Reduction of the crystallization rate of HDPE in the presence of Induced Condensing Agents

Fabiana N. Andrade[a], René Fulchiron[b], Franck Collas [c], Timothy F.L. McKenna[a*]

[a] C2P2-UMR 5265, Université de Lyon, Bâtiment ESCPE, 43 Blvd du 11 Novembre 1918, F-69616 Villeurbanne, France

[b] CNRS UMR 5223, Université de Lyon, Ingénierie des Matériaux Polymères, F-69622 Villeurbanne, France

[c] Mettler Toledo, 18/20 avenue de la Pépinière, F-78222 Viroflay France

[*] Author to whom correspondence may be addressed: timothy.mckenna@univ-lyon1.fr

ABSTRACT

The crystallization of high-density polyethylene (HDPE) alone, and in the presence of n-hexane (a common induced condensing agent – ICA) was studied using Differential Scanning Calorimetry (DSC). The presence of a non-crystallizable ICA which is partially soluble in the amorphous phase of HDPE reduces the rate of crystallization. This was reflected by a shifting of the crystallization and melting peaks of HDPE to lower temperatures when the ICA concentration in the medium increases. It is also observed that the rate of crystallization of HDPE can be very slow when the ratio of ICA to HDPE increases from zero. This behavior is useful to better understand the physical effects that can potentially occur at the beginning of the gas phase polymerization of ethylene, and suggests that the crystallization of the nascent polymer, and thus the properties of the polymer in the reactor will be quite different from those of the powder at later stages of the reaction when running in condensed mode.

Keywords: induced condensing agents (ICA); isothermal crystallization; high density polyethylene; kinetic of crystallization.

1 Introduction

High density polyethylene (HDPE) can be produced on an industrial scale using different types of processes, the two most widely used being in diluent slurry and a gas phase. In a gas phase process, the polymerization takes place in a continuous fluidized bed reactor (FBR), where a gas mixture is brought into contact with a supported catalyst. The mixture typically is composed of ethylene, hydrogen, variable amounts of comonomers such as 1-butene or 1-hexene, inert gases to regulate partial pressures, and eventually alkanes to help with heat transfer. These last compounds are often referred to as induced condensing agents (ICA), and are often isomers of butane, pentane, and hexane [1–3].

The monomer(s) diffuse from the continuous phase into the pores of the solid catalyst particles, where they then polymerize at the active sites situated therein. As polymer builds up, it creates hydraulic tensions that provoke the rupture or fragmentation of the original support [4–6]. The morphology of the final particles will depend strongly on this fragmentation step because the way in which the particles rupture represents a trade-off between the rate of generation of stress caused by the polymerization on the one hand, and the ability of the particle to dissipate the mechanical energy on the other [7–9]. Thus, the physical properties of the polymer during this part of the polymerization, and in particular the crystallinity [10] can have a strong influence on fragmentation. In addition, the crystallinity can influence monomer solubility [11], as well as the rates of diffusion [12] through the growing polymer particle [13–15]. These last two quantities (solubility and diffusivity of penetrants) will also be a function of the type and quantity of ICA added to the reactor. For instance, it has recently been shown that adding up to 0.8 bars of n-hexane to a gas phase polymerization of ethylene can lead to a significant enhancement of both monomer diffusivity and reaction rate with respect to what is observed for a polymerization in the absence of ICA [16]. The authors of this last work noted

that the greatest deviation between experiment and model predictions was at the beginning of the reaction, where the free-volume based model apparently underestimated the effective diffusivity of ethylene in the amorphous polymer in the presence of n-hexane. It is entirely possible that this is because the fraction of amorphous material is underestimated during this phase of the polymerization. This in turns begs the question about how fast the formation of crystals is with respect to the formation of polymer chains – in other words, can we assume that the crystallinity of the nascent polymer is similar to that of the final reactor powder?

Note also that laboratory scale polymerization of ethylene in the presence of an ICA (pentant or hexane) revealed that adding the ICA led to the formation of an HDPE that had a higher degree of crystallinity than a polymer made with ethylene alone under otherwise identical conditions. In addition, adding the ICA also led to significant increases in the average molecular weight of HDPE.[16] The increase in the average molecular weight can be (at least in large part) attributed to an increase in the ethylene concentration at the active sites due to the comonomer effect, and the higher crystallinity in the presence of an ICA was mainly attributed to the mechanism of crystallization of polymer chains in the presence of solubilized ICA which can act to promote solvent vapor annealing [17]. It is possible that this combination of rapidly forming chains and higher molecular weight leads to a slowing down of the crystallization process, allowing the chains more time to reorganize and form more crystalline polymers.

The crystallization of the polymer is governed by the extent and type of branching, the comonomer composition, and external factors such as the presence of plasticizers like ICA. In general, the crystallization of polymers is a kinetic phenomenon: in the molten state, all of the polymer chains are disordered (amorphous), and they need time to organize in an ordered

structure (crystalline polymer). There will therefore be a characteristic time for chain crystallization, just as there is a characteristic time for chain formation.

All of these points suggest that it would be useful for us to understand what, if any, influence the presence of an ICA has the rate of crystallization during PE production – is it rapid with respect to the fraction of a second that the polymer chains grow? Or is it a slower process?

Polymer crystallization theory

Whenever particles crystallize out of solution, two fundamental processes are involved: crystal nucleation and growth. A unified theory of crystallization does not exist, but a set of complementary theories have been developed that can help us to understand the impact of sorbed alkanes on PE crystallization. Morphological theories generally calculate an equilibrium morphology based on the energetic interactions of different crystal faces in order to estimate its final form, and thus do not take into consideration the nucleation phase, which is in fact useful to understand the role that ICA might play in crystallization [18–20]. All morphological theories consider two barriers to crystal growth: one that accounts for the thermodynamic barrier to include a crystalline stem on the growing lamella, and another that accounts for the diffusion of a molecule towards the lamella. Inclusion of a stem into a growing crystal is enhanced by decreasing temperatures whereas the second barrier becomes more significant. The purpose here is not to discuss the differences between the theories, but rather to understand the points they have in common to assess what affects the rate of crystallization. Moreover, for temperatures far above the glass transition temperature (T_g), which is the case in the present work, polymer diffusion is fast enough that it is not the limiting mechanism. Therefore, only the crystalline stem deposit mechanism has to be considered.

In this case, the crystallization rate is controlled by the free energy difference between the liquid and the solid phases. This difference is commonly considered proportional to the degree of supercooling, represented by the difference between the equilibrium melting temperature (T_m^0) and the temperature at which we are observing the system. T_m^0 is the temperature at which the crystal would melt if it was of infinite dimensions, [21] and it is thus the limiting temperature for the crystallization process. More rarely, a "zero growth" temperature instead of T_m^0 is considered as the limit [22]. Regardless of the definition chosen, crystallization kinetics are governed by the temperature difference between this limiting temperature and the actual crystallization temperature, and this degree of supercooling is in the denominator of a negative exponential function. This means that a small variation of the supercooling drastically modifies the crystallization kinetics. In addition to the crystallization temperature, the crystallization kinetics can be alternatively modified by the concentration of a diluent that alters the equilibrium melting temperature. [23]

This last point can be illustrated using Flory-Huggins theory to calculate the free energy of the fringed micelle model, in which the crystallization processes occur only when the system is supersaturated. In general, supersaturation can be imposed on a system by cooling, solvent evaporation, the addition of an anti-solvent or by chemical reaction [24]. Supersaturation is the driving force of the crystallization process, meaning that crystallization occurs only if the system is supersaturated. This implies that in order for a crystallization process to occur spontaneously, it needs to be accompanied by decrease in the free energy. Thus the increase of entropy due to presence of a diluent means that T_m^0 decreases, and this must be compensated for by a decrease in the crystallization temperature. The Flory-Huggins

136 equation describes this dependence of the equilibrium melt temperature on the concentration
137 of a diluent [25].
138
139 Figure 1 shows the relationship of the free energy with temperature, where it compares the
140 effect of the presence of the diluent on the free energy. The equilibrium melt temperature will
141 be lower for a dilute system, and this has been observed in the case of polyethylene in the
142 presence of heavier alkanes [26], xylenes and o-dichlorobenzene [27–29], and other diluents [25,30,31].
143 Teymouri et. al. [32] evaluated LDPE and n-hexane thermograms with different swelling times
144 and observed that although there were no major changes in equilibrium melt temperature,
145 therewas a significant shift in the lowest melt peak in the presence of the solvent (from 90 ºC
146 for pure LDPE to 70 °C for LDPE swollen by Hexane). It was observed that the rate of
147 crystallization decreased at temperatures near the melting point, and was kinetically
148 controlled under thermodynamic conditions far from equilibrium [33]. Some kinetic studies of
149 polyethylene with xylene [34] and o-dichlorobenzene [35], show that the rate of crystallization
150 decreases as we approach the melting point.

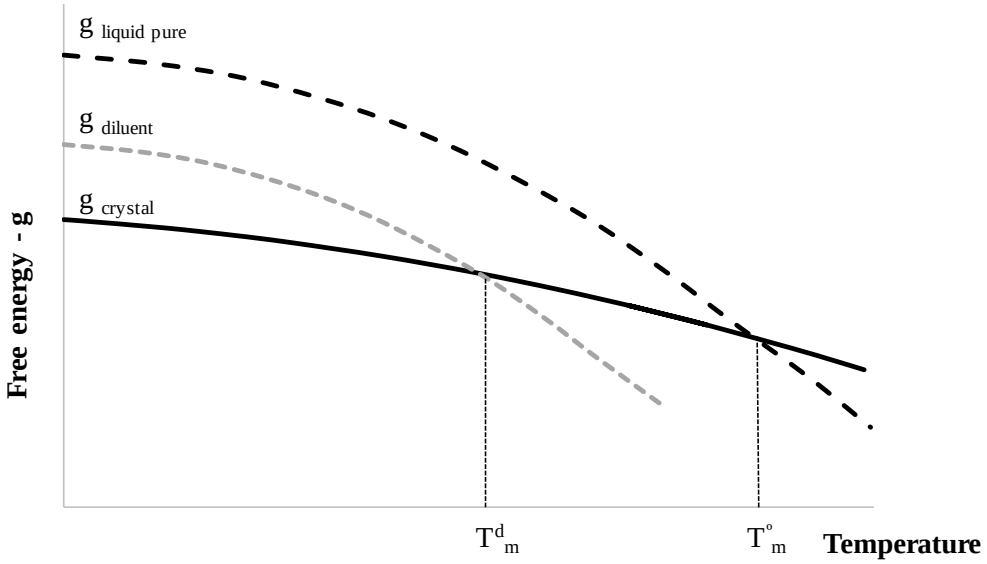

151

152 Figure 1 - Relation between free energy and temperature for pure polymer and diluent systems.
153

If one considers crystallization caused by cooling, it can be assumed that crystallization in the presence of a diluent will occur for an equivalent degree of supercooling with respect to the crystallization temperature of pure polymer.

In conclusion, since the presence of alkanes in of polyethylene causes a decrease in the equilibrium melting temperature, it must also lead to a depression of the crystallization temperature and rate. It is therefore possible that the crystallization rate of polyethylene is slower in the presence of an ICA (with respect of a system without ICA) at temperatures between 90 - 115 °C.

2 Experimental section

2.1 Materials

The high-density polyethylene (HDPE) used in this work was produced in gas phase polymerization experiments performed in the spherical stirred-bed semi batch reactor, as described elsewhere[15]. Polymerizations were run at a pressure of 7 bars of ethylene at 70 ºC without hydrogen and 80 ºC in presence of 1 and 3 bar hydrogen. Molecular weight data are shown in Table 1. N-Hexane was used as the induced condensing agent (minimum purity 99%, from Sigma-Aldrich ICN - Germany). The ICA properties are shown in Table 2.

Table 1. HDPE types

Samples [a)]	$T_{reactor}$	$P_{Ethylene}$	$P_{Hydrogen}$	**Yield**	M_n	M_w	M_z
	°C	**bar g**	**bar g**	$g_{pol}.g_{cat}^{-1}$	**kg.mol^{-1}**	**kg.mol^{-1}**	**kg.mol^{-1}**
HDPE70	70	7	0	1,575	114	751	2,936
HDPE-1H_2	80	7	1	2,158	59	278	955
HDPE-3H_2	80	7	3	1,312	33	145	448

a) The sample name is identified by HDPE + polymerization temperature [°C]

Table 2. ICA proprieties

ICA	P^{vap} bar 70 – 120 °C	BP °C at 1 atm	M_w kg. mol^{-1}
n-Hexane	1.034 – 3.987	69	86.18

2.2 Preparation of sample blends

In order to evaluate the impact of ICA on the crystallization process, HDPE and blends of HDPE plus different levels of ICA were placed in 120 μL medium pressure steel capsules, and analyzed by DSC. In the case of the blends, a given mass (5 - 20 mg) of HDPE was weighed and placed in the medium pressure capsule. Then a specific volume (varying from 10 - 60 μL) of n-hexane (ICA) was added to the capsule using a micropipette. Due to the volatile nature of n-hexane, the amount of ICA finally enclosed in the capsule was determined gravimetrically. The capsules were weighed before and after the DSC analyses to verify if any ICA had evaporated during the procedure, thus correcting the ICA mass. These limits of polymer weight plus ICA concentration were chosen to represent different moments in the semi-bath, lab scale polymerization process. Note that in a semi-batch reactor the ratio of ICA to polymer is actually quite high during the very early stages of polymerization (zero polymer in a salt seed bed at the beginning of polymerization), and decreases as polymer is formed.

2.3 Differential Scanning Calorimetry (DSC)

The DSC analyses were carried out using a Mettler Toledo DSC 3+ model in two different ways: i) an non-isothermal evaluation of the impact of different blend composition on the

crystallization temperatures and degree of crystallinity of the polymer samples; ii) a study of the isothermal crystallization kinetics to assess the crystallization times at different values of T_c. The ICA concentration in the blends for each study phase is shown in Table 3.

Table 3. ICA:HDPE blends (weight percent ICA:HDPE)

Samples	**Non-isothermal**	**Isothermal**
HDPE70	0 – 22 – 87 – 99 – 99.8 %	0 – 17 – 25 – 85 %
HDPE-1H_2	-	0 – 15 – 28 – 86 %
HDPE-3H_2	-	0 – 15 – 28 – 86 %

All analyses were performed under a nitrogen atmosphere - 30 mL/min. The following procedure was used for the non-isothermal analyses:

(i) Cooling of the sample from room temperature to -20 °C at a rate of 10 °C / min;

(ii) Heating from -20 °C to 180 °C at a rate of 2 °C / min;

(iii) Isothermal hold at 180 °C for 120 min;

(iv) Cooling from 180 °C to -20 °C with rates of 2 °C / min;

(v) Isothermal hold at -20 °C for 120 min;

(vi) Heating from -20 °C to 180 °C at a rate of 2 °C / min.

The parameters of interest in the first non-isothermal studies are the range of crystallization temperatures (T_c), melting temperatures (T_m - corresponding to the second heating), total heat of crystallization (Q_c - measurement of the area under the endotherm divided by the polymer mass in the blend), total heat of fusion (Q_m - measurement of the area under the exotherm also divided by the polymer mass in the blend), and degree of crystallinity (w_c - calculated in relation to 100% crystalline HDPE).

The isothermal crystallization of the ICA+HDPE mixtures was performed at different crystallization temperatures (T_c). The procedure starts by cooling the sample from room temperature to -20 °C at a rate of 10 °C / min and continues with a cycle of five sequential steps:

(i) Heating from -20 °C to 180 °C at a rate of 2 °C / min;

(ii) Cooling from 180 °C to T_c at rates of 50 °C / min;

(iii) Isothermal hold at T_c for 120 min;

(iv) T_c cooling to -20 °C with rates of 10 °C / min;

(v) Heating from -20 °C to 180 °C at a rate of 2 °C / min.

T_c values of 91, 94, 97, 100 and 115 °C were employed in this study. The thermograms were analyzed to obtain the time and degree of crystallization for a given T_c isotherm, and the melting temperature.

All data obtained in the analysis were from the thermograms treated using STARe Software Evaluation, version 14.00. The enthalpy of 100% crystalline polymer was taken as $\Delta H° = 293$ J / g [36]. For validation, the method was repeated for different concentrations of the blend, such as HDPE70-85% for the non-isothermal and HDPE70-1%, HDPE70-80% for the isothermal. All runs showed a standard deviation of less than 10%.

3 Results and discussions

Non-isothermal analyses

In the first series of experiments, the non-isothermal evolution of the crystallization and melting points of the different mixtures of HDPE and ICA are shown in Figure 2, and a

summary of the properties of these same runs are presented in Table 4. If one considers the thermograms in Figure 2, it is immediately (and perhaps intuitively) obvious that the crystallization temperature of mixtures of HDPE and ICA decrease as the relative concentration of the latter increases. As pointed out by Yamamoto [33], the rate of crystallization decreases as the system approaches its melting point. In other words, one might suspect from these results that the characteristic time for crystallization would be different in the samples with different ICA:HDPE ratios.

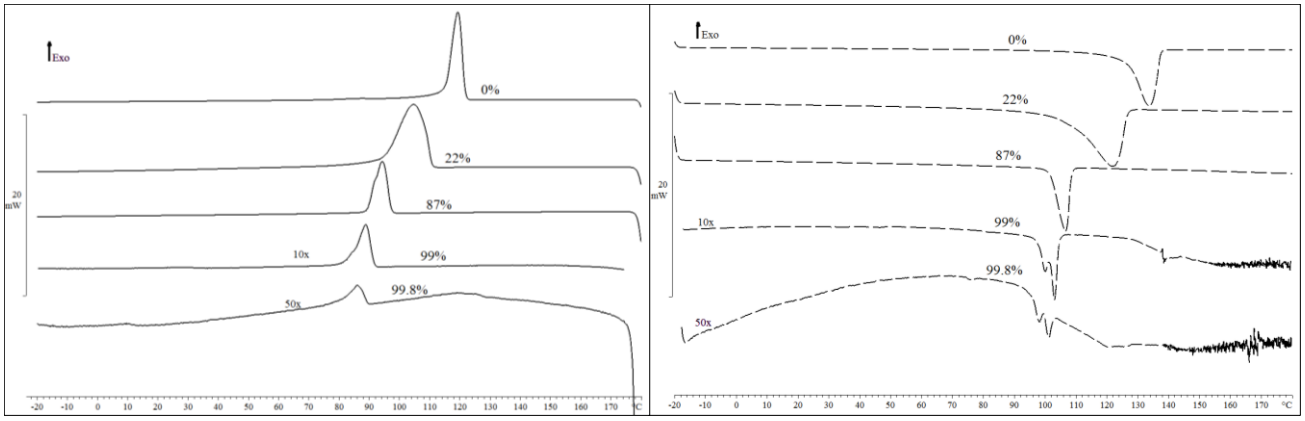

Figure 2 - Non-isothermal thermograms from HDPE70 samples: Left are the peaks of the exothermic crystallization curves (T_c) and right are the peaks of the endothermic melting curves (2a heating – (T_m). The curve size of the 99% blend is multiplied by ten, and for the blend 99.8% is multiplied by fifty.

In addition, and as shown in Table 4, all the samples show the same (expected) tendencies with the increase of ICA concentration in the blends:

- T_c and T_m, estimated by the peak of the exothermic and endothermic curves respectively, decrease. T_m decreases by 33 °C over the range of compositions studied, and T_c by 34°C in the case of HDPE70;

- There is an increase in the total heat of crystallization (Q_c), of melting (Q_m), and of the degree of crystallinity (w_c). At high ICA to polymer ratios, the polymer is almost entirely crystalline at the end of the cooling step.

Note that in case of very diluted system, it can be reasonably assumed that there is no longer entanglement between polymer chains, entanglements which would be trapped and excluded from the crystallizable entities. Hence, the final attainable crystallinity is higher.

The difference between Q_c and Q_m remained approximately invariant, which shows that the presence of ICA has a very strong influence on the total amount of crystalline phase in the polymer, the HDPE that recrystallizes from dilute solutions having a higher overall crystallinity than those recrystallizing from solutions more concentrated in polymer.

Table 4. Parameters obtained from the thermograms

Samples	Parameters	ICA:HDPE blends				
HDPE70	y_{ICA}	**0%**	**22%**	**87%**	**99%**	**99.8%**
	$y_{polymer}$	100%	78%	13%	1%	0.2%
	w_c (%)	**55.7**	**56.2**	**67.5**	**86.3**	**97.3**
	T_c on (°C)	122	111	97	92	90
	T_c peak (°C)	120	105	95	89	86
	T_c end (°C)	115	95	90	84	82
	T_m (°C)	134	122	106	103	101
	Q_c (J / g)	163	165	198	253	285
	Q_m (J / g)	-165	-165	-197	-250	-282
	ΔQ_{m-c}	1.2%	0.3%	0.5%	1.1%	1.1%

Figure 3a shows that the melting point depression is more pronounced when there is more ICA in the capsule, as expected [37]. Figure 3b shows the peak of the crystallization temperature and the crystallization range. It can be seen from this figure that crystallization can be seen at

temperatures below 100 °C for blends containing more than 20% ICA. For levels of less than 20% ICA by weight, the range is around 115 - 122 °C.

These initial observations support the idea that when ICA are present during the nascent stage of polymerization in a semi batch reactor, they can promote a decrease in rate of crystallization during the first instants of the polymerization before significant levels of polymer begin to accumulate, and the equilibrium melt temperature can eventually approach the temperature of the reactor.

In order to better understand the behavior of the crystallization rate, the isotherms were evaluated in the range 90 - 115 ºC for comparison of the different blends. An isotherm at 130 ºC (chosen as no crystallization is expected at this temperature) was also measured and used to subtract any imperfections from the curves analyzed.

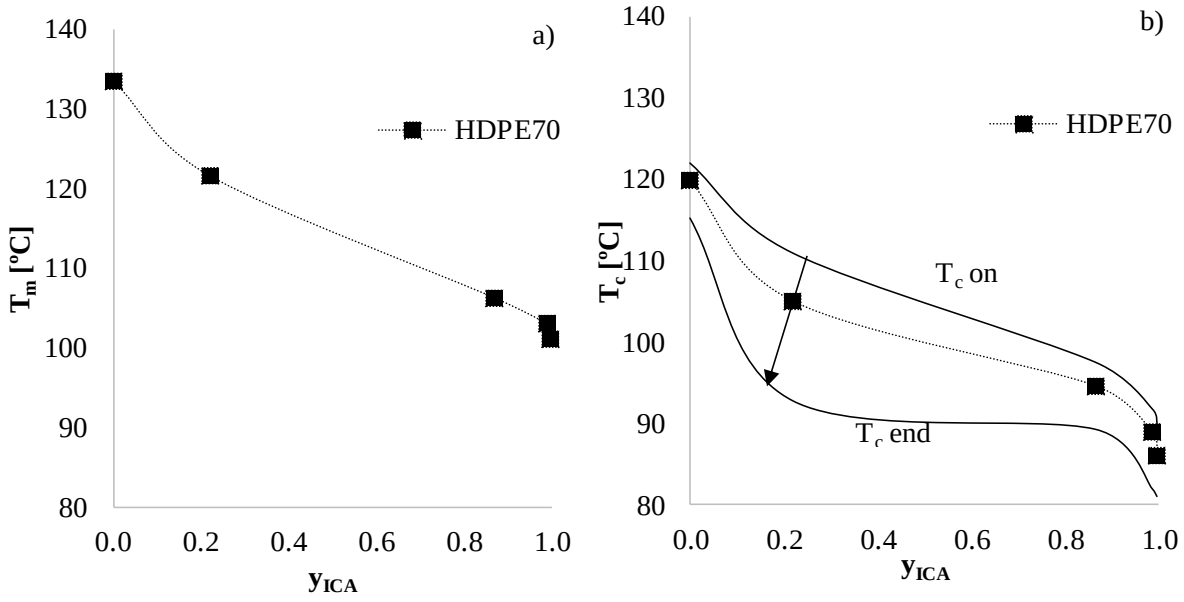

Figure 3 - a) Melt temperature and b) Crystallization temperature as a function of the mass fraction of ICA in an ICA-HDPE mixture

Isothermal analyses

The isotherms used in this part of the study began after abrupt cooling. According to Zhang et al. [36] if the cooling is rapid enough under the right conditions, there is not sufficient time for crystal nucleation and growth. We therefore considered that the quantity of crystallization that occurred during the cooling phase was negligible, and that the vast majority crystallization occurred during the isothermal phase. Nevertheless, when the degree of supercooling is high enough, the crystallization can be quite rapid. Even though we used the cooling rate of 50 °C / min, a preliminary study showed that some of the samples might begin to crystallize during the initial phase cooling before the temperature is stabilized. Thus we will only present results for the pure polymer and 17% ICA:HDPE at T_c = 115 °C, 25% ICA:HDPE at T_c = 100 °C and 85% ICA:HDPE at T_c = 94 °C, and for samples of polymers with hydrogen (lower molecular weight) at T_c = 115 °C. The ICA in each blend can be solubilized in the amorphous phase of the available polymer mass and also present as a vapor. If enough ICA is present, it can be also be present as a separate liquid phase.

From the data obtained by DSC, the study of crystallization kinetics was carried out using the classical model of Avrami [38,39] and an evaluation of the equilibrium melt temperature (T_m^0) with the procedure of Hoffman and Weeks [40].

The Avrami approach aims at calculating the volume of material that crystallizes as a function of time. The model states that the crystallinity developed by a heated isothermal material for a time t can be correlated with the type and kinetics of nucleation and crystalline growth. The main assumptions on which the Avrami equation is based are that the sample is large enough to neglect the edge effects, the nuclei distribution is spatially random, and the activation of the nuclei and the growth rate of the crystalline lamellae are independent of time (the last two

assumptions being verified in isothermal mode). This model, described by equation 1, provides parameters for the kinetics of total crystallization under isothermal conditions [36,41].

$$\alpha(t) = 1 - \exp(-kt^n) \qquad \text{Equation 1}$$

Where $\alpha(t)$ is the relative (fractional) crystallinity as a function of time, and n and k are the Avrami parameters. n is related to the type of nucleation, morphology, and size of crystals developed during crystallization, and k is related to the nucleation rate and growth of the crystalline phase. The evaluation of the relative crystallinity as a function of time is carried out from the ratio between the partial (at time t) and total areas of the crystallization isotherm (in relation to the baseline, which represents the zero-heat flux), generating a typical sigmoidal curve. By plotting equation 1 in double log form, we obtain a straight line whose slope gives the values of n, and the intercept (at log(t) = 0) gives the values of k.

All isotherms shown in Figures 4 and 5 have a sigmoid shape characteristic of a phase transformation process. The results show that an increase of T_c corresponded to a shift to longer crystallization times, indicating a decrease in the rate of crystallization for all of the blends studied with respect to pure polymer. This is a consequence of reducing the supercooling, thus reducing the driving force of the crystallization process. Analyzing the specific behavior of the mixtures (Figure 4) at 0 and 17% of ICA at T_c = 115 °C (all ICA absorbed in the polymer), and as the ICA concentration in the capsule increases (corresponding to the presence of a liquid phase) it was found that the presence of ICA affects the crystallization behavior of the polymer, both in terms of the temperature and the time of crystallization. It is clear that the blends have a much slower crystallization relative to the pure polymer. The hexane molecules act as a diluent, slowing down the crystallization process

by modifying the liquid free energy (see Figure 1) and consequently reducing the supercooling for a given crystallization temperature. Table 6 shows a significant increase of the *t½* values observe (the time it takes to reach 50% of the total crystallization for a given sample blend) in the presence of ICA.

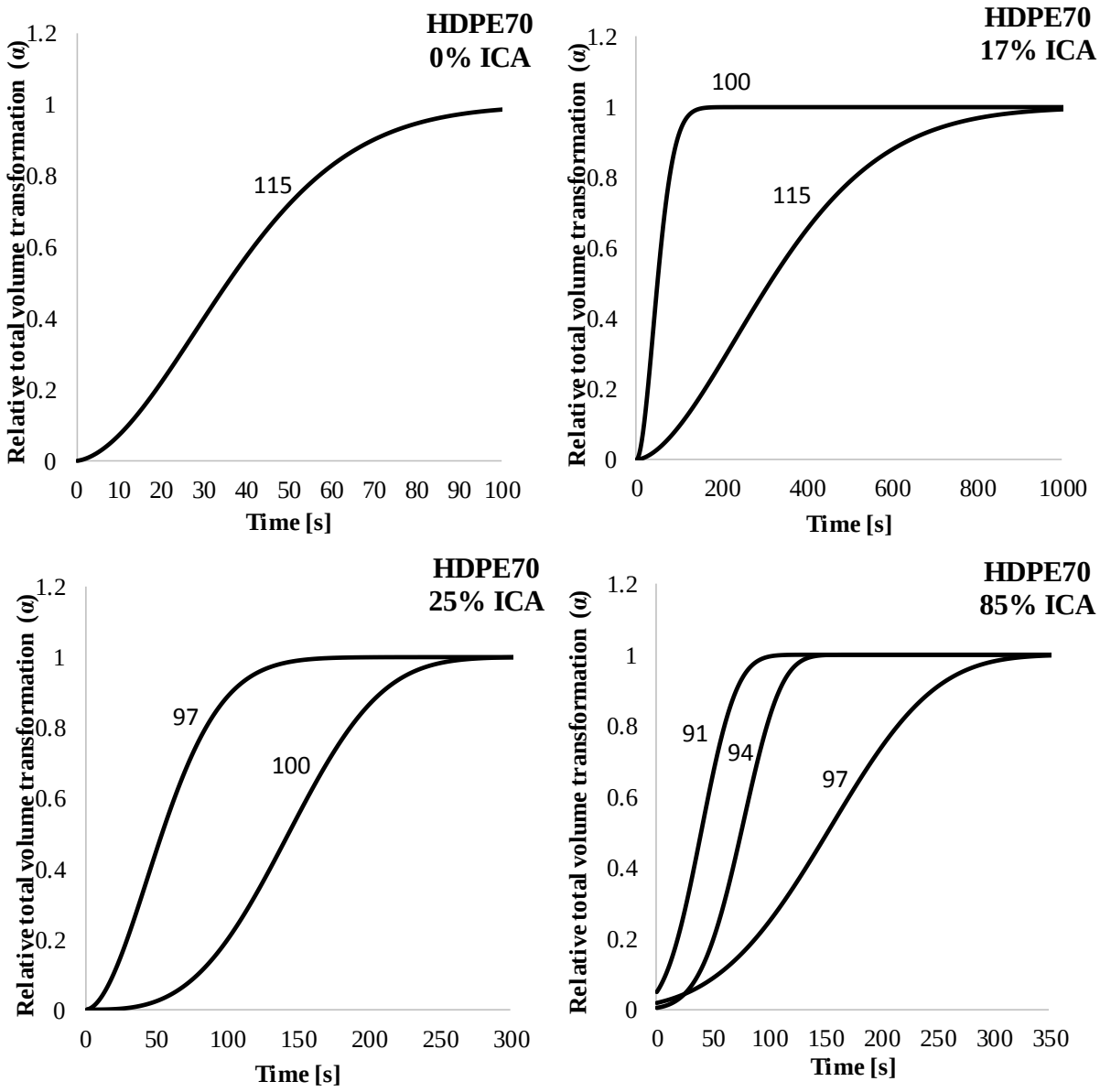

Figure 4 - Relative crystallinity curves for HDPE70 blends samples at different T_c [°C]

When we evaluate the impact of the molecular weight on the rate of crystallization, we see that the crystallization time increases as the molecular weight increses. HDPE-1H_2 (278 kDa) and HDPE-3H_2 (145 kDa) pure, 15% ICA:HDPE-H_2 and 86% ICA:HDPE-H_2, the

crystallization time is faster for the lower molecular weight polymer. However, 28% ICA:HDPE-H_2 exhibit almost the same behavior (Figure 5). Indeed, for such dilution, the decrease in molecular mobility caused by an increase of molecular weight is negligible. The variation of $t½$ as a function of molecular weight is displayed in Table 6.

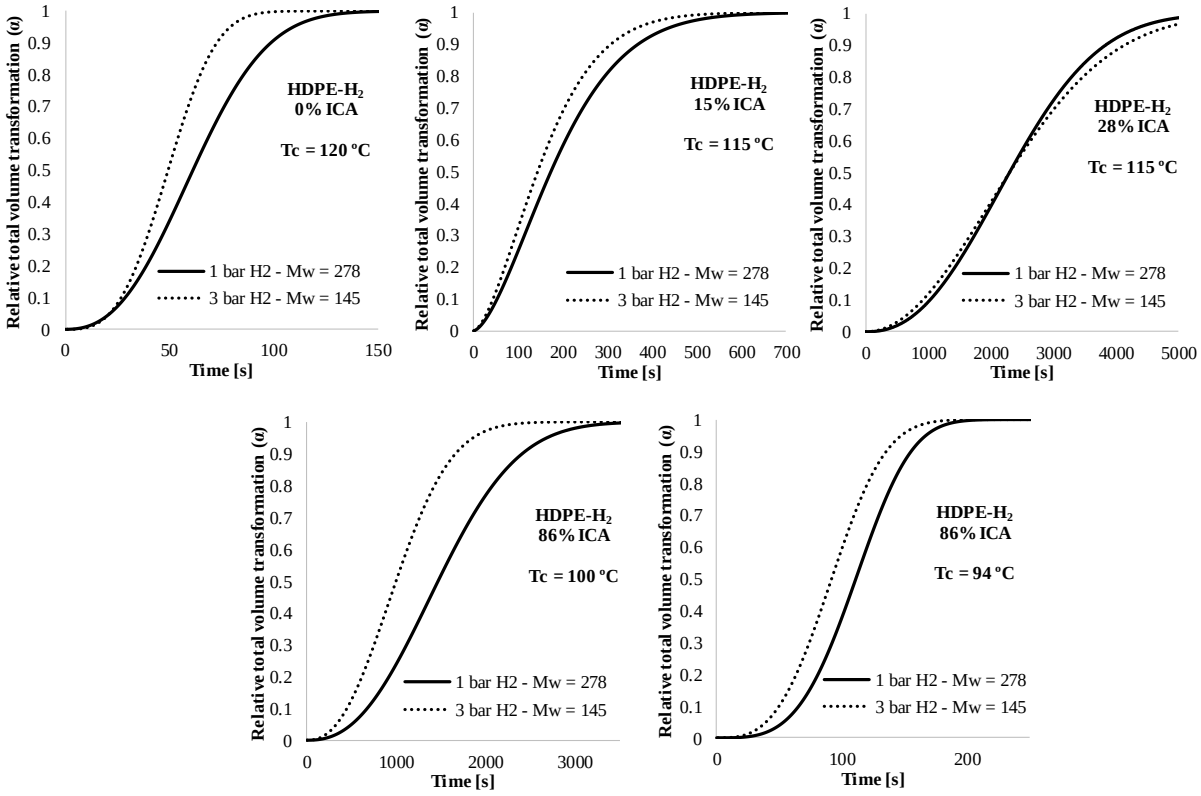

Figure 5 - Relative crystallinity curves for HDPE70 blends samples at different T_c [°C]

A study of the melting behavior of the samples in the presence of ICA was then performed on the samples that were isothermally crystallized at different temperatures. The melting occurs over a wide range of temperatures because of different sizes and degrees of perfection of the crystals present. If T_m is defined as the peak of the curve, its value does not truly represent an intrinsic property of the material. For this reason, T_m^o, which represents the melting temperature of infinitely large crystals, constitutes a more appropriate parameter for evaluating the differences in thermal stability of the various compositions [39].

The calculation of T_m^o was performed according to the Hoffman-Weeks procedure, in which the measured melting temperature T_m (obtained in the last step of the thermal characterization procedure) of each isothermally crystallized sample is plotted against its T_c. The line of equation $T_m = T_c$ is also plotted and the intersection of the two lines gives the value of T_m^o.

Table 5. Time of half crystallization - *t½*.

T_c [ºC]	HDPE70				HDPE-1H_2				HDPE-3H_2			
	0%	17%	25%	85%	0%	15%	28%	86%	0%	15%	28%	86%
91				73								
94				108				112				92
97			54	240				322				212
100		49	143					1470				998
115	36	313				174	2.303			143	2.303	
120					62				49			

The evaluation of T_m° according to the Hoffman-Weeks method (Figure 5.5), allows one to compare T_m° of the pure HDPE with that of the blends. For pure HDPE average value of T_m° is approximately 135.5 ºC. While this value it is lower than the theoretical melting point for HDPE ($T_m^\circ \approx 142$ ºC [40]), this value lies within the range 133 - 138 ºC typically observed for real HDPE [42]. These differences are due to possible experimental error, but all points present errors less than 5%. T_m° for blends of ICA and HDPE is lower than that of pure HDPE, typically near 130 °C for 15-17% ICA:HDPE, and 110 °C for 85% ICA:HDPE. A decrease in the equilibrium melting temperature is observed for both two samples. This shows that there is miscibility between HDPE and ICA.

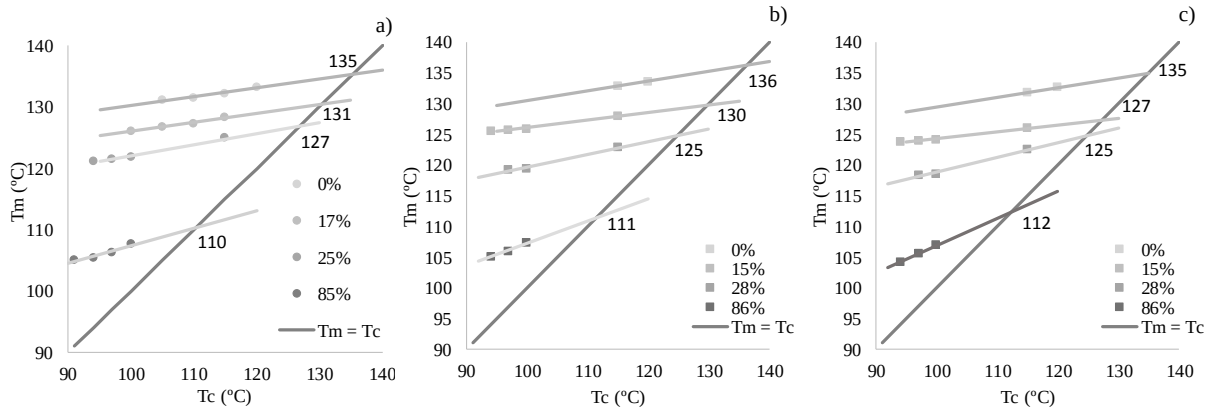

Figura 6 - Determination of Tmº by the Hoffman-Weeks method. a) HDPE70 - fraction ICA. b) HDPE-1H2 - fraction ICA. c) HDPE-3H2 - fraction ICA.

Considering the Flory-Huggins theory, the equilibrium melting temperature variation with the diluent concentration can be expressed by:

$$\frac{1}{T_m^0} - \frac{1}{T_{m,melt}^0} = \frac{RV_u}{\Delta h_u V_d}(\phi_d - \chi\phi_d^2) \qquad \text{Equation 2}$$

where T^0_m and $T^0_{m,melt}$ are the equilibrium melting temperatures of respectively the polymer in solution and the bulk polymer $T^0_{m,melt}$ =414.6K and V_d is the molar volume of the diluent (for hexane this is 113 Å^3), V_u is the molar volume of the repeat unit (for ethylene 38 Å^3) [43], ΔH_u is the heat of fusion of the repeat unit (4,096 J.mol^{-1}), ϕ_d is the volume fraction of the diluent in the blend and χ is the Flory-Huggins interaction parameter. An interaction parameter value lower than 0.5 indicates a total miscibility while the miscibility is only partial for χ greater than 0.5. The experimental equilibrium melting temperature was considered in equation.

Figure 7, the obtained values of T^0_m are plotted against the volume fraction of ICA. Clearly (especially for HDPE 70), a value of χ lower than 0.5 leads to a theoretical description of the equilibrium melting temperature for all ICA fractions. This leads to the conclusion that (as

one would expect) the PE and ICA are totally miscible over range of ICA fractions investigated here.

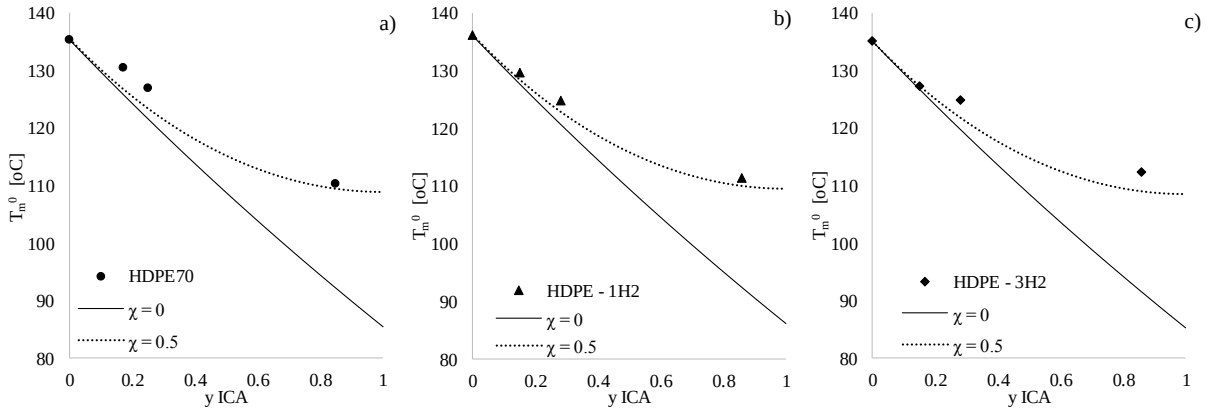

Figura 7 - Evaluation Flory equation. a) HDPE70 - fraction ICA. b) HDPE-1H_2 - fraction ICA. c) HDPE-3H_2 - fraction ICA.

4 Conclusions

In the current study, the isothermal crystallization kinetics of blends of n-hexane and HDPE were analyzed by differential scanning calorimetry. The main conclusions are summarized below:

- ICA:HDPE ratios form miscible blends
- An equilibrium melt temperature depression (i.e. lower T_m), and an increase in the attainable crystallinity of HDPE were observed with increasing quantities of ICA;
- The crystallization time is significantly higher for the blends compared to the pure polymer.

The impact on the crystallization time could have a significant impact on several process-related issues. First of all, if a virgin catalyst particle is injected into the reactor without prepolymerization, the ratio of ICA to polymer on the particle will be very high as the initial chains are formed. This means that the diffusivity and solubility of ethylene will be higher

during the initial instants, and thus the concentration of monomer at the active sites and rate of polymerization will also be higher with respect to polymer formed on "mature" particles. This is important, especially if we wish to interpret lab-scale data in terms of a kinetic model, since it is essential to be able to distinguish between physical phenomena (e.g. sorption or diffusion) and intrinsic catalyst kinetics.

In addition, the slower crystallization rate in the presence of ICA implies that the polymer particles can, in some instances undergo a fragmentation step where the polymer is essentially all amorphous in the presence of ICA, whereas in dry mode, it is possible that the polymer crystallizes much more quickly and the particle fragmentation (and transport processes) is quite different in dry mode. One also suspects the melting point depression caused by the ICA would lead the fresh particles to be much stickier than the "older" ones, and perhaps increase the possibility of agglomeration in the reactor.

Finally, while slurry phase polymerization has not been discussed in the current paper, it should be clear from the results presented here that polymer swelling, crystallization and morphogenesis will all probably be quite different if one compares slurry to gas phase processes.

Acknowledgements: Financial support of this work from the National Council of Scientific and Technological Development (CNPq), branch of the Ministry of Science, Technology, Innovation and Communications (MCTIC) of Brazil.

Received: XXXX XX, 2018; Revised: Month XX, XXXX; Published online:

((For PPP, use “Accepted: Month XX, XXXX” instead of “Published online”)); DOI: 10.1002/marc.((insert number)) ((or ppap., mabi., macp., mame., mren., mats.))

TOC

The crystallization rate of high-density polyethylene (HDPE) was studied using Differential Scanning Calorimetry (DSC), and it was shown that the presence of an alkane (or induced condensing agent) reduces the rate of polymer crystallization, in some cases to time scales on the order of minutes under conditions characteristic of lab-scale experiments.

References

(1) J. R. Parrish, G. A. Lambert, D. N. Thomas, "Gas Phase Polymerization and Method of Controlling Same," Patent US 7625987 B2, **2009**.

(2) R. Y. Banat, F. Al-Obaidi, A. K. Malek, "Olefin Gas Phase Polymerisation," US 2013/0066027 A1, **2013**.

(3) R. Y. Banat, F. Al-Obaidi, A. K. Malek, "Olefin Gas Phase Polymerisation," US 2014/0148563 A1, **2014**.

(4) W. L. Carrick; G. L. Karapinka; R. J. Millington. Polymerization Process. US 3324095, **1967**.

(5) H. B. Irvin; F. T. Sherk. Polyolefin Reactor System. US 4121029, **1978**.

(6) A. R. Miller. Fluidized Bed Reactor. US 4003712, **1977**.

(7) T. F. L. McKenna, A. Di Martino, G. Weickert, J. B. P. Soares. Particle Growth during the Polymerisation of Olefins on Supported Catalysts, 1 - Nascent Polymer Structures. *Macromol. React. Eng. 4* (1), 40–64, **2010**.

(8) A. Di Martino, G. Weickert, F. Sidoroff, T. F. L. McKenna. Modelling Induced Tension in a Growing Catalyst/Polyolefin Particle: A Multi-Scale Approach for Simplified Morphology Modelling. *Macromol. React. Eng. 1* (3), 338–352, **2007**.

(9) B. Horáčková, Z. Grof, J. Kosek. Dynamics of Fragmentation of Catalyst Carriers in Catalytic Polymerization of Olefins. *Chem. Eng. Sci. 62* (18–20), 5264–5270, **2007**.

(10) A. Alizadeh, T. F. L. McKenna. Particle Growth during the Polymerization of Olefins on Supported Catalysts. Part 2: Current Experimental Understanding and Modeling Progresses on Particle Fragmentation, Growth, and Morphology Development. *Macromol. React. Eng. 12* (1), **2018**.

(11) V. Kanellopoulos, D. Mouratides, P. Pladis, C. Kiparissides. Prediction of Solubility of α-Olefins in Polyolefins Using a Combined Equation of State - Molecular Dynamics Approach. *Ind. Eng. Chem. Res. 45* (17), 5870–5878, **2006**.

(12) A. G. Fisch, J. H. Z. dos Santos, N. S. M. Cardozo, A. R. Secchi. Mass Transfer in Olefin Polymerization: Estimative of Macro- and Microscale Diffusion Coefficients through the Swollen Polymer. *Chem. Eng. Sci. 63* (14), 3727–3739, **2008**.

(13) M. Namkajorn, A. Alizadeh, E. Somsook, T. F. L. McKenna. Condensed Mode Cooling for Ethylene Polymerisation : The Influence of Inert Condensing Agent on the Polymerisation Rate. *Macromol. Chem. Phys. 1918* (215), 873–878, **2014**.

(14) A. Alizadeh, M. Namkajorn, E. Somsook, T. F. L. McKenna. Condensed Mode

Cooling for Ethylene Polymerization: Part II. From Cosolubility to Comonomer and Hydrogen Effects. *Macromol. Chem. Phys.* No. 216, 985–995, **2015**.

(15) F. N. Andrade, T. F. L. McKenna. Condensed Mode Cooling for Ethylene Polymerization: Part IV. The Effect of Temperature in the Presence of Induced Condensing Agents. *Macromol. Chem. Phys. 218* (20), 1–8, **2017**.

(16) M. Namkajorn, A. Alizadeh, D. Romano, S. Rastogi, T. F. L. McKenna. Condensed Mode Cooling for Ethylene Polymerization: Part III. The Impact of Induced Condensing Agents on Particle Morphology and Polymer Properties. *Macromol. Chem. Phys. 217* (13), 1521–1528, **2016**.

(17) J. Mark, K. Ngai, W. Graessley, L. Mandelkern, E. Samulski, J. Koenig and G. Wignall. *Physical Properties of Polymers*, Third Ed.; Cambridge University Press, **2003**.

(18) R. Boistelle, J. P. Astier. Crystallization Mechanisms in Solution. *J. Cryst. Growth 90* (1–3), 14–30, **1988**.

(19) R. J. Kirkpatrick, Crystal Growth from the Melt: A Review. *Am. Miner. 60*, 798–814, **1975**.

(20) M. Zhang, B.-H. Guo, J. Xu. A Review on Polymer Crystallization Theories. *Crystals*; Vol. 7, 4, **2017**.

(21) J. D. Hoffman, R. L. Miller. Kinetic of Crystallization from the Melt and Chain Folding in Polyethylene Fractions Revisited: Theory and Experiment. *Polymer. 38* (13), 3151–3212, **1997**.

(22) G. Strobl, T. Y. Cho. Growth Kinetics of Polymer Crystals in Bulk. *Eur. Phys. J. E 23* (1), 55–65, **2007**.

(23) L. Mandelkern, A. L. Allou Jr. The fusion of polyethylene single crystals. Academic Press, *Polymers, 4 447-452,* **1973**.

(24) A. G. Jones, Crystallization Process Systems. *Cryst. Process Syst.* 341, **2002**.

(25) F. Toquet, L. Guy, B. Schlegel, P. Cassagnau, R. Fulchiron. Effect of the Naphthenic Oil and Precipitated Silica on the Crystallization of Ultrahigh-Molecular-Weight Polyethylene. *Polym. (United Kingdom) 97*, 63–68, **2016**.

(26) A. Nalcajima, F. Hamada. Estimation of Thermodynamic Interactions between Polyethylene and N-Alkanes by Means of Melting Point Measurements. *Kolloid-Zeitsehrift und Zeitschrift fiir Polymere, Band 205 82*, 55- 61, **1965**.

(27) G. Valdecasas, The Crystallization of Polymer-Diluent Mixtures. *J. Polym. Sci. Phys*

13, 2103–2115 **1975**.

(28) E. Riande, J. M. G. Fatou. Effect of Solvent on the Crystallization from Dilute Polyethylene Solutions. *Polymer. 17* (9), 795–801, **1976**.

(29) E. Riande, J. M. G. Fatou. Crystallzation of Dilute Polyethylene Solutions: Influence of Molecular Weight. *Polymer. 17*, 99–104, **1976**.

(30) E. Riande, J. M. G. Fatou. Crystallization Kinetics of Polyethylene Paraffin Mixtures. *19*, 1295–1299, **1978**.

(31) W. Cobbs Jr, R. Burton. Crystallization of Polyethylene Terephthalate. *J. Polym. Sci. 10* (3), 275–290, **1953**.

(32) Y. Teymouri, A. Adams, B. Blümich. Compact Low-Field NMR: Unmasking Morphological Changes from Solvent-Induced Crystallization in Polyethylene. *Eur. Polym. J. 80*, 48–57, **2016**.

(33) T. Yamamoto. Computer Modeling of Polymer Crystallization - Toward Computer-Assisted Materials' Design. *Polymer 50* (9), 1975–1985, **2009**.

(34) A. J. McHugh, W. R. Burghardt, D. A. Holland. The Kinetics and Morphology of Polyethylene Solution Crystallization. *Polymer. 27* (10), 1585–1594, **1986**.

(35) S. Chew, J. R. Griffiths, Z. H. Starchurski. The Crystallization Kinetics of Polyethylene under Isothermal and Non-Isothermal Conditions. *Polymer 30* (5), 874–881, **1989**.

(36) J. Zhang, S. Chen, J. Su, X. Shi, J. Jin, X. Wang, Z. Xu. Non-Isothermal Crystallization Kinetics and Melting Behavior of EAA with Different Acrylic Acid Content. *J. Therm. Anal. Calorim. 97* (3), 959–967, **2009**.

(37) T. F. L. McKenna. Condensed Mode Cooling of Ethylene Polymerization in Fluidized Bed Reactors. *Macromol. React. Eng. 1800026*, **2018**.

(38) Z. Zhang, F. Yu, H. Zhang. Isothermal and Non-Isothermal Crystallization Studies of Long Chain Branched Polypropylene Containing Poly(Ethylene-Co-Octene) under Quiescent and Shear Conditions. *Polymers (Basel). 9* (6), **2017**.

(39) H. Marand, J. Xu, S. Srinivas. Determination of the Equilibrium Melting Temperature of Polymer Crystals: Linear and Nonlinear Hoffman-Weeks Extrapolations. *Macromolecules 31* (23), 8219–8229, **1998**.

(40) J. D. Hoffman, J. J. Weeks. Melting Process and the Equilibrium Melting Temperature of Polychlorotrifluoroethylene. *J. Res. Natl. Bur. Stand. Sect. A Phys. Chem. 66A* (1), 13–28, **1962**.

(41) E. Koscher, R. Fulchiron. Influence of Shear on Polypropylene Crystallization:

582 Morphology Development and Kinetics. *Polymer 43* (25), 6931–6942, **2002**.
583 (42) E. Benham, M. McDaniel. Polyethylene, High Density; 2004; Vol. **1936**.
584 (43) Anesthetic Structure Database | Ethene (Ethylene)
585 http://asd.molfield.org/php/view_details.php?id=45&java=false (accessed Nov 23, **2018**).
586